

# Photometric and H $\alpha$ observations of LSI+61 $^{\circ}$ 303: detection of a $\sim$ 26 day V and JHK band modulation

J. M. Paredes<sup>1,2</sup>, P. Marziani<sup>3</sup>, J. Martí<sup>1</sup>, J. Fabregat<sup>4</sup>, M. J. Coe<sup>5</sup>, C. Everall<sup>5</sup>, F. Figueras<sup>1,2</sup>, C. Jordi<sup>1,2</sup>, A. J. Norton<sup>6</sup>, T. Prince<sup>7</sup>, V. Reglero<sup>4</sup>, P. Roche<sup>5</sup>, J. Torra<sup>1,2</sup>, S. J. Unger<sup>6</sup>, and R. Zamanov<sup>8</sup>

<sup>1</sup> Departament d'Astronomia i Meteorologia, Universitat de Barcelona, Av. Diagonal 647, E-08028 Barcelona, Spain

<sup>2</sup> And Laboratori d'Astrofísica, Societat Catalana de Física (IEC), Spain

<sup>3</sup> Department of Physics & Astronomy, University of Alabama, Tuscaloosa AL 35487-0324, USA

<sup>4</sup> Departamento de Matemática Aplicada y Astronomía, Universidad de Valencia, 46100 Burjassot, Valencia, Spain

<sup>5</sup> Physics Department, University of Southampton, Southampton SO9 5NH, UK

<sup>6</sup> Department of Physics, The Open University, Walton Hall, Milton Keynes MK7 6AA, UK

<sup>7</sup> Division of Physics, Mathematics and Astronomy, Caltech, Pasadena, CA 91125, USA

<sup>8</sup> National Astronomical Observatory Rozhen, POB 136, 4700 Smoljan, Bulgaria

Received ; Accepted

## Abstract.

We present new optical and infrared photometric observations and high resolution H $\alpha$  spectra of the periodic radio star LSI+61 $^{\circ}$ 303. The optical photometric data set covers the time interval 1985-1993 and amounts to about a hundred nights. A period of  $\sim$ 26 days is found in the V band. The infrared data also present evidence for a similar periodicity, but with higher amplitude of variation ( $0^m.2$ ). The spectroscopic observations include 16 intermediate and high dispersion spectra of LSI+61 $^{\circ}$ 303 collected between January 1989 and February 1993. The H $\alpha$  emission line profile and its variations are analyzed. Several emission line parameters – among them the H $\alpha$  EW and the width of the H $\alpha$  red hump – change strongly at or close to radio maximum, and may exhibit periodic variability. We also observe a significant change in the peak separation. The H $\alpha$  profile of LSI+61 $^{\circ}$ 303 does not seem peculiar for a Be star. However, several of the observed variations of the H $\alpha$  profile can probably be associated with the presence of the compact, secondary star.

**Key words:** Stars: LSI+61 $^{\circ}$ 303 – Stars: emission line, Be – Stars: variables – Radio continuum: stars – X-ray: stars

## 1. Introduction

The early-type star LSI+61 $^{\circ}$ 303 (V 615 Cas) is the optical counterpart of the variable radio source GT 0236+610, discovered during a galactic plane radio survey (Gregory & Taylor, 1978). Taylor & Gregory (1982) found that this object exhibits strong radio outbursts with a 26.5 d period. Further observations (Taylor & Gregory, 1984) established the currently accepted value of  $26.496 \pm 0.008$  d. Typically, radio outbursts

peak around phases 0.6-0.8 (Paredes et al., 1990). The spectroscopic radial velocity observations of Hutchings & Crampton (1981), hereafter HC81, are in agreement with the radio period, and give support to the presence of a companion. In addition, they also conclude that the optical spectrum corresponds to a rapidly rotating B0 V star, with an equatorial disk and mass loss.

All the radio data available to date on the outburst peak flux density provide evidence for a strong modulation, over a time scale of 4 yr, in the amplitude of the 26.5 d periodic radio outbursts (Gregory et al., 1989; Paredes et al., 1990; Estalella et al., 1993). The dependence of radio outbursts flux density on frequency, the peak time delay, and the general shape of the radio light curves can be modeled as continuous relativistic particle injection into an adiabatically expanding synchrotron emitting source (Paredes et al., 1991). Furthermore, recent VLBI observations have provided the first high resolution map of LSI+61 $^{\circ}$ 303 showing a double sub-arcsec structure (Massi et al., 1993). The physical parameters derived from these VLBI observations and those of Taylor et al. (1992) are in agreement with this model.

The system was detected as an X-ray source by Bignami et al. (1981) and has also been proposed (Gregory & Taylor, 1978; Perotti et al., 1980) to be the radio counterpart of the COS B  $\gamma$ -ray source CG135+01 (Hersem et al., 1977). However, this last association is still doubtful due to the large  $\gamma$ -ray error box.

Paredes & Figueras (1986) based on UBVR photometric observations detected optical variability roughly correlated with the radio light curve. The amplitude was about  $0^m.1$ . A model based on deformations of the primary star by a compact companion in an eccentric system was initially applied by Paredes (1987) to explain it. Optical variability with time scales of days has also been reported by Lipunova (1988) who, in addition, found short term nightly fluctuations of some hundredths of a magnitude. These short time fluctuations were first observed by Bartolini et al. (1983). More recently, Mendelson &

Send offprint requests to: J. M. Paredes

Mazeh (1989) reported an optical modulation with amplitude similar to that found by Paredes & Figueras (1986) and with a period of  $26.62 \pm 0.09$  d, near to the radio value, in the Johnson I band. However, their data set was not sufficient to show clearly a similar periodicity at shorter wavelengths.

The photometric results presented in this paper confirm that a  $\sim 26$  d periodicity is actually present in the V band. In addition, the general shape of the visual light curve is very similar to that observed by Mendelson & Mazeh (1989) in the I band. In the JHK near infrared bands, we find clear evidence that a similar periodic modulation is also present, with amplitude of  $\sim 0^m.2$ .

On the other hand, intermediate resolution spectroscopic data of LSI+61°303 suitable for an analysis of the H $\alpha$  emission line profile are available in literature, at the time of writing, only from the early papers of Gregory et al. (1979) and HC81. These papers outlined the variations of the H $\alpha$  profile, but were far from reaching any firm conclusion regarding the mechanism responsible for such variations. In this work, we present 16 spectra (9 of them of high resolution, 0.2-0.44 Å FWHM) obtained with linear detectors. The new spectra allow a more detailed description of the H $\alpha$  line profile and of its variation. We confirm many of the early findings of Gregory et al. (1979) and of HC81 concerning line shifts and H $\alpha$  EW variations. Moreover, we find that other intriguing changes in the H $\alpha$  line profile (noticeably the width of the red hump) occur at or close to radio outburst.

## 2. Photometric observations and results

The Johnson photometric observations were made at Calar Alto (Almería, Spain) with the 1.23 m telescope of the Centro Astronómico Hispano-Alemán (CAHA) and the 1.52 m telescope of the Observatorio Astronómico Nacional (OAN) and at the Observatorio del Roque de los Muchachos (ORM, La Palma, Spain), using the 1 m Jacobus Kapteyn telescope (JKT). They cover the period 1985-1993 and amount to one hundred independent photometric measurements. Both Calar Alto telescopes are equipped with a one channel photometer with a dry-ice cooled RCA 31034 photomultiplier. The JKT observations were made using the People's photometer, with two channels, which is equipped with EMI 9658AM photomultipliers.

The differential photometry was performed using SAO 12319 (V=8.79 and I=7.76), SAO 12327 (V=8.15 and I=6.90) and BD+60°493 (V=8.41 and I=7.04) as comparison stars. The majority of measurements were obtained in the Johnson V filter, although some simultaneous I filter observations were also taken and will be reported here. Differences of magnitude between comparison stars themselves are constant within  $0^m.02$ . Further details of the observing technique are reported in Paredes & Figueras (1986).

The infrared observations were made at the Teide Observatory, (Tenerife, Spain), using the 1.5 m Carlos Sánchez telescope (TCS) equipped with the continuously variable filter (CVF) photometer. The data were corrected for atmospheric extinction and flux-calibrated by comparison with an adequate sample of standard stars.

The results of our Johnson photometric observations are given in Table 1. First column indicates the Julian date, second and third column are, respectively, the Johnson V and I band magnitudes of LSI+61°303. A similar format has been used for

the infrared observations, whose results are presented in Table 2. Figure 1 shows, with the same scale, the optical and infrared full data set folded with the radio period of 26.496 d.

## 3. Photometric analysis

### 3.1. V Photometric periodicity

In order to try to confirm independently the periodic optical modulation reported by Mendelson & Mazeh (1989), a period analysis was carried out over this entire data set, amounting to 105 photometric V measurements over the time interval 1985-1993. The period analysis of the data was performed by using the phase dispersion minimization (PDM) technique (Stellingwerf, 1978). This method consists of assuming a trial period and then constructing a phase diagram. The phase interval is divided into bins and the variance of the data points is computed in each bin. The weighted mean of the variances is divided by the total variance of the data. It can be shown that local minima of this function correspond to periods present in the data or to multiples of such periods.

Considering that our minimum sampling rate is about one day, our period search was made up to a frequency of  $0.5 \text{ c d}^{-1}$ . The result of PDM analysis of the V band data is shown in Fig. 2. The most significant minimum in the explored frequency range (from 0.01 to  $0.5 \text{ c d}^{-1}$ ) occurs on  $0.0387 \text{ c d}^{-1}$  and the uncertainty that we associate with this frequency is the frequency resolution of the complete data set, given by  $\sim 1/T$ , where  $T$  is the total length of the data span and is equal to  $0.0004 \text{ c d}^{-1}$ . This corresponds to a period of  $25.8 \pm 0.3$  d.

From this analysis, it appears evident that a modulation with period of  $\sim 26$  d is actually present in the Johnson V photometry of LSI+61°303. This period is similar to that of 26.62 d found by Mendelson & Mazeh (1989) in the Johnson I band and to the 26.496 d radio periodicity (Taylor & Gregory, 1984). In Fig. 3 we have plotted our 105 photometric V points folded on the 26.496 d radio period and binned into 10 bins. Error bars indicate the formal estimate of the uncertainty of the mean within each bin. For clarity, the data are plotted twice. From this figure we note the similar shape with the optical light curves presented by Mendelson & Mazeh (1989). In particular, the presence of a broad brightness maximum near radio active phases 0.5-0.9, and a clear minimum around phase 0.3 can be appreciated.

Once the existence of an optical modulation with a period near to 26 d has been established in an independent way from Mendelson & Mazeh (1989), it is worth carrying out an analysis of all long term photometric data available today for LSI+61°303. In this way, we have searched for periodicities, in the range from 20 to 30 d, the ensemble consisting of both our data and the photometric points published by Bartolini et al. (1983), Lipunova (1988) and Mendelson & Mazeh (1989), amounting to 204 nights. Using a frequency step of  $2 \times 10^{-7} \text{ c d}^{-1}$  and a bin structure (5,2), the deepest PDM minimum corresponds to  $26.5 \pm 0.2$  d, although it is not very prominent. This period value is coincident with the radio period.

### 3.2. I Photometry

Our set of Johnson I band observations, listed in Table 1, amount to 43 nights only. With this small data set, it is not possible to carry out a feasible periodicity search. In Fig. 1, we

**Table 1.** Johnson photometric observations of LSI+61°303

Julian Date (2440000+)	V	I	Julian Day (2440000+)	V	I
6264.62	10.74	9.26	7452.68	10.76	-
6265.59	10.74	9.25	7456.44	10.77	-
6267.55	10.75	9.24	7456.63	10.77	-
6268.58	10.70	9.20	7802.60	10.77	9.31
6269.61	10.72	9.20	7803.61	10.78	9.32
6270.62	10.65	9.14	7804.60	10.79	9.31
6271.60	10.71	9.20	7805.59	10.77	9.29
6272.60	10.70	9.19	7806.64	10.77	9.29
6273.61	10.74	9.23	7807.64	10.77	9.28
6274.60	10.74	9.24	7808.62	10.77	9.29
6421.52	10.77	9.30	7809.59	10.76	9.27
6423.34	10.73	9.28	7833.67	10.75	9.28
7056.45	10.76	9.27	7837.59	10.74	9.29
7058.43	10.74	9.24	7838.56	10.72	9.28
7060.58	10.76	9.27	7957.34	10.74	9.32
7063.57	10.73	9.24	8176.43	10.75	9.30
7069.64	10.72	9.21	8180.38	10.74	9.28
7096.66	10.64	-	8238.30	10.76	9.31
7097.56	10.65	-	8274.46	10.79	-
7098.64	10.70	-	8275.49	10.79	-
7125.35	10.68	-	8474.69	10.79	9.28
7128.30	10.67	-	8527.46	10.75	9.29
7147.30	10.75	-	8545.53	10.78	-
7148.30	10.76	-	8620.50	10.75	-
7149.59	10.71	-	8898.65	10.76	9.29
7151.40	10.73	-	9003.46	10.74	9.28
7152.43	10.72	-	9004.47	10.75	9.29
7169.28	10.74	-	9005.45	10.75	9.28
7170.45	10.70	-	7125.35	10.67	-
7169.54	10.71	-	7128.30	10.68	-
7171.56	10.67	-	7168.43	10.80	-
7172.35	10.71	-	7169.30	10.78	-
7172.57	10.64	-	7170.44	10.78	-
7231.34	10.74	-	7367.64	10.75	-
7232.35	10.70	-	7368.64	10.80	-
7381.65	10.74	-	7531.32	10.73	-
7381.65	10.74	-	8092.58	10.77	-
7388.63	10.79	-	8194.49	10.71	-
7389.59	10.78	-	8207.51	10.76	-
7390.59	10.77	-	8208.42	10.74	-
7391.64	10.77	-	8209.35	10.70	-
7392.67	10.78	-	8262.55	10.75	9.31
7393.59	10.78	-	8266.31	10.73	9.31
7394.59	10.75	-	8267.31	10.74	9.28
7395.65	10.76	-	8268.30	10.74	9.33
7420.54	10.70	-	8270.31	10.76	9.34
7421.52	10.74	-	8577.53	10.79	-
7422.56	10.74	-	8610.38	10.76	-
7422.69	10.74	-	8611.41	10.76	-
7423.65	10.77	-	8962.45	10.79	-
7424.64	10.79	-	9034.40	10.74	-
7425.59	10.79	-	9034.40	10.69	-
7426.62	10.78	-			

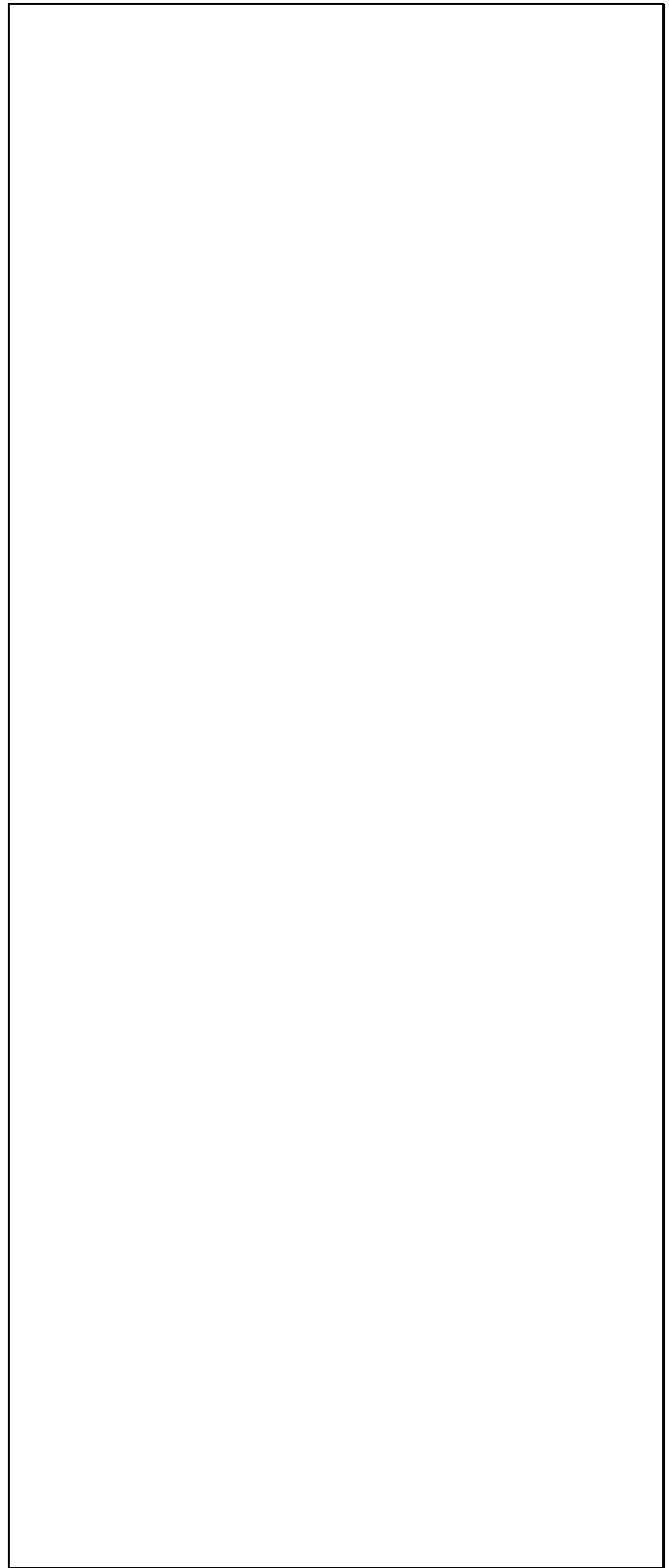


**Fig. 1.** Optical and infrared observations of LSI+61°303 folded on the 26.496 d radio period. Phase zero has been set at JD 2443366.775 (Taylor & Gregory, 1982). From top to bottom, the V, I, J, H, and K band are plotted. The dots at phase 0.7 are from Elias et al. (1985). All observations are plotted twice.

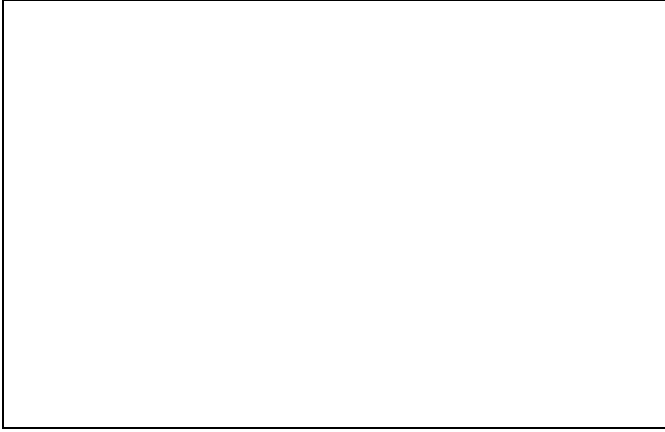


**Fig. 2.** PDM periodogram of the V band data with bin structure (5,5) and frequency step  $5 \times 10^{-5}$  c d $^{-1}$ . The frequencies are in cycles per day. The deepest minimum occurs at a frequency of  $0.0387$  c d $^{-1}$ , corresponding to a period of 25.8 d.

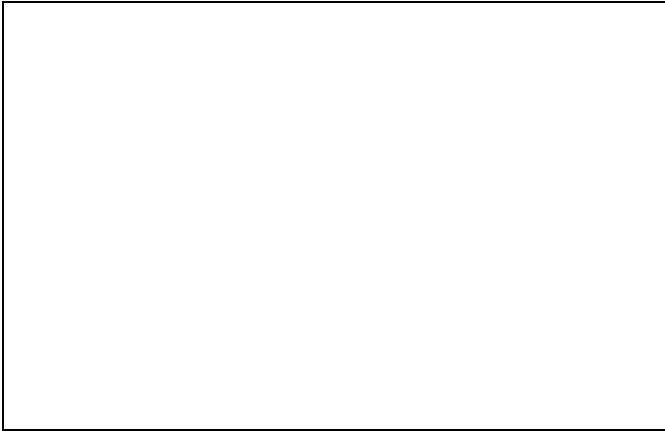


**Fig. 3.** Bin average V light curve of LSI+61°303 folded on the 26.496 d radio period. Phase zero has been set at JD 2443366.775 (Taylor & Gregory, 1982). Errors bars indicate the formal estimate of the uncertainty of the mean within each bin. The continuous line is plotted for visual aid. All data is plotted twice.

show the I band observations folded with the 26.496 d radio period. The available data covers the phase interval 0.2-0.9. However, this partial light curve presents the same trends as that of V band observations. In particular, a maximum near the central radio phases and low emission level near phase 0.2 is clearly seen.

### 3.3. JHK bands photometric periodicity

Our JHK photometric observations are plotted in Fig. 1 as a function of radio phase. Also, we have included two points (dots) at phase  $\sim 0.7$  observed by Elias et al. (1985). The infrared data available have a good coverage over the full radio period, and indicates that the infrared light curves of LSI+61°303 also present a modulation similar to that of V and I bands. However, the infrared high emission state (orbital phases  $\sim 0.6-0.9$ ) is broader than in the optical, while the minimum emission state (orbital phases  $\sim 0.2-0.4$ ) is deeper and narrower.

**Table 2.** JHKL' photometric observations of LSI+61°303

Julian Day (2440000+)	J	H	K	L'
7161.46	8.76	8.39	8.06	-
7163.45	8.81	8.39	8.13	7.60
7164.38	8.77	8.38	8.15	7.59
8279.45	8.73	8.32	8.03	-
9013.47	8.62	8.25	7.88	-
8284.51	8.60	8.30	7.90	-
8491.59	8.74	8.34	8.04	-
8493.57	8.80	8.35	8.05	-
8494.60	8.68	8.26	7.97	-
8496.55	8.62	8.22	7.91	-
8498.51	8.57	8.18	7.87	-
8590.35	8.70	8.20	7.90	-
8592.47	8.71	8.29	8.01	-
8665.42	8.57	8.16	7.89	-
8669.46	8.60	8.25	7.96	-
8856.65	8.66	8.20	7.88	-
8857.67	8.62	8.21	7.92	-
8858.65	8.62	8.19	7.92	-

For a single infrared band, the amount of data accumulated by us, 18 nights, could not suffice to carry out a significant period search. In order to overcome this problem, we have merged all the JHK photometric points after subtracting their respective mean and dividing by the corresponding r.m.s. dispersion in each filter. This process is roughly equivalent to having a very broad bandpass filter, about  $1\mu\text{m}$  wide. The two points observed by Elias et al. (1985) have also been included. This provides a data set of relative normalized infrared magnitudes, with 60 measurements over which we have carried a PDM period analysis. The minimum sampling rate is about one day. So, the PDM search was carried out up to a frequency of  $0.5$  c d $^{-1}$ . The result of PDM analysis of the merged JHK band data is shown in Fig. 4. The most prominent minimum occurs on  $0.0370 \pm 0.0003$  c d $^{-1}$ , corresponding to a period of  $27.0 \pm 0.3$  d. Another nearby deep minimum, with comparable significance, is found at  $0.0376 \pm 0.0003$  c d $^{-1}$ , corresponding to a period of  $26.6 \pm 0.3$  d. This implies that an infrared modulation, with period similar to the radio period, is also present in LSI+61°303. The 60 normalized points used are plotted in Fig. 5 as a function of radio phase, computed using the radio period value of 26.496 d.

### 3.4. Photometric discussion

The JHK infrared light curves of Fig. 1, showing a deep minimum at phase  $\sim 0.3$  and a rather flat maximum centered around phase  $\sim 0.8$ , are reminiscent of light curves from eclipsing variables. From a rotation velocity value of  $v \sin i \simeq 360 \pm 25$  km s $^{-1}$ , HC81 suggest that orbital inclination of LSI+61°303 is close to  $90^\circ$ . So, this makes the eclipse possibility a rather reasonable interpretation.

In addition, the existence of an IR excess in LSI+61°303 has been reported by D'Amico et al. (1987) and Elias et al.

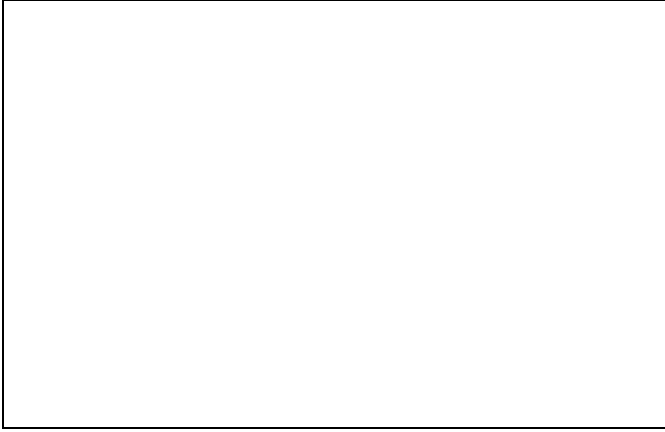


**Fig. 4.** PDM periodogram of the merged JHK band data with bin structure (5,5) and frequency step  $5 \times 10^{-5} \text{ c d}^{-1}$ . The frequencies are in cycles per day. The deepest minimum occurs at a frequency of  $0.0370 \text{ c d}^{-1}$ , corresponding to a period of 27.0 d.

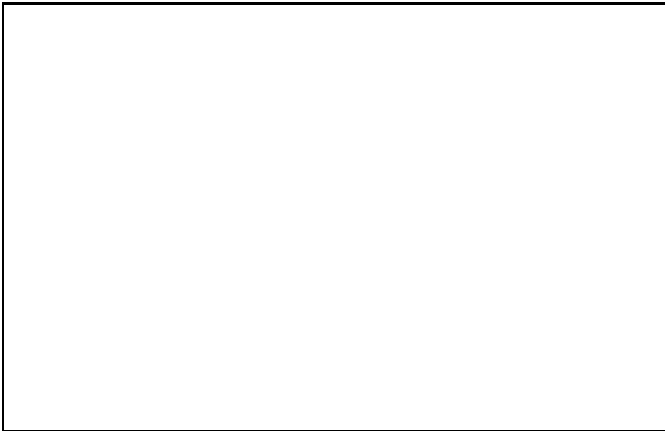


**Fig. 5.** JHK infrared observations of LSI+61°303 after subtracting the mean magnitude of each filter and normalizing with their respective r.m.s. dispersion. They are shown folded on the 26.496 d radio period. Phase zero has been set at JD 2443366.775. All observations are plotted twice.

(1985). This is, however, a rather common situation in Be stars, where the IR excess at micron wavelengths is attributed to a dense circumstellar envelope (Slettebak, 1979). This envelope can be also partially responsible for the  $H\alpha$  emission. Due to the presence of this envelope, its free-free and free-bound opacity is also very likely to absorb the infrared radiation from any orbiting companion, thus strongly influencing the observed light curve beyond a simple geometrical eclipse. A theoretical modelling of the JHK light curves, based on this eclipse-attenuation scenario, could yield a determination of the system orbital parameters (Martí & Paredes, 1994).

On the other hand, when considering the optical light curves, one sees that the minimum is wider and lasts for about half an orbital cycle (see Fig. 3). Then, as suggested by Mendelson & Mazeh (1989), the eclipse explanation at these wavelengths is more difficult to accept. However, due to the approximate frequency dependence  $\tau_\nu \propto \nu^{-3}$ , the optical free-free and free-bound extinction is actually very low. So, any attenuation effects will be difficult to appreciate in the optical

band, meaning that optical variability should be accounted for by a different physical mechanism, probably involving X-ray heating of parts of the normal star facing the X-ray source.

#### 4. Spectroscopic observations and results

Sixteen spectra covering the  $H\alpha$  spectral range were collected during several observing runs from January 1989 to February 1993. Table 3 reports the dates of observation and basic information on the instrumental setup. The first column indicates the spectrum identification, the second and third the observatory and telescope used, the fourth, fifth and sixth contain the date, UT time and Julian day of observation, respectively. Seventh column is the radio phase. Finally, the eighth and ninth columns indicate the dispersion and covered spectral range. All spectra were recorded employing CCD detectors. They were bias subtracted and flat field corrected using the IRAF or FIGARO package, with the exception of Rozhen spectra which have been reduced using the pcIPS software package (Smirnov et al., 1992). Only the spectrum obtained on Dec. 27, 1990 (LP1, see Table 3) at La Palma was flux calibrated.

In Fig. 6 we show our normalized  $H\alpha$  record of LSI+61°303 ordered sequentially with radio phase and drawn on the same scale with an arbitrary offset. For days with multiple measurements, only the best profile is shown. The continuum underlying  $H\alpha$  was rectified to unity employing a spline fitting. This normalization procedure is somewhat arbitrary for Rozhen Observatory spectra, since the spectral range covered is very small, and since most of the  $H\alpha$  wings is probably lost in noise.

The  $H\alpha$  line profile of LSI+61°303 shows broad wings as well as a double peaked core. The Full Width Zero Intensity (FWZI) of  $H\alpha$  measured on the Mt. Palomar spectra is  $\approx 3100 \text{ km s}^{-1}$ . In addition, in the Asiago spectra, the red hump is nearly flat topped and shows a broad shoulder to the red.

Line parameters were measured on each normalized spectrum and are reported in Table 4. First column gives the spectrum identification. Second, third and fourth columns list the heliocentric radial velocity of the blue peak, central dip, and red peak, respectively. Fifth and sixth columns are the FWHM of the blue and red hump, corrected for instrumental profile, while seventh column provides the ratio between the blue and red peak intensity above continuum. Eighth column gives the total  $H\alpha$  EW and the ninth column lists the EW of the wings. Finally, the tenth column contains the EW ratio of the red and blue humps.

The radial velocity, the FWHM and the peak height of the B and R humps were measured employing a gaussian fitting. In the high resolution spectra, the fitting was done after rebinning to a dispersion of  $\sim 1 \text{ \AA/pixel}$ . We estimated the contribution of the wings by subtracting from the  $H\alpha$  profile a model of the core composed of two gaussians.

#### 5. Spectroscopic analysis

##### 5.1. Radial velocities

In Fig. 7, we show the radial velocity difference between the R and B peaks as well as the central dip radial velocity, both as a function of radio phase. The velocity difference between the  $H\alpha$  peaks reaches a maximum close to the radio outburst, during an interval of two tenths of radio phase. On the other hand, Gregory et al. (1979) noted already that the Balmer central dip varied within the range  $-30/-80 \text{ km s}^{-1}$  over the period

**Table 3.** Summary of spectroscopic observations of LSI+61°303

Id.	Observatory	Telescope	Date	UT	Julian Day (2440000+)	Radio Phase	Dispersion (Å/pix)	Spectral Range (Å)
AS1	Asiago	1.8m	1989 Jan 18	19 <sup>h</sup> 29 <sup>m</sup>	7545.3	0.70	0.22	6513-6650
AS2	Asiago	1.8m	1989 Jan 19	19 <sup>h</sup> 27 <sup>m</sup>	7546.3	0.74	0.22	6510-6652
AS3	Asiago	1.8m	1989 Jan 19	20 <sup>h</sup> 21 <sup>m</sup>	7546.3	0.74	0.22	6510-6652
AS4	Asiago	1.8m	1989 Jan 21	19 <sup>h</sup> 55 <sup>m</sup>	7548.3	0.82	0.22	6510-6652
AS5	Asiago	1.8m	1989 Jan 21	20 <sup>h</sup> 47 <sup>m</sup>	7548.4	0.82	0.22	6510-6652
LP1	La Palma	2.5m	1990 Dec 27	01 <sup>h</sup> 14 <sup>m</sup>	8252.5	0.40	0.38	6492-6672
LP2	La Palma	2.5m	1991 Jan 27	23 <sup>h</sup> 18 <sup>m</sup>	8283.5	0.57	0.78	6400-6800
LP3	La Palma	2.5m	1991 Aug 28	02 <sup>h</sup> 05 <sup>m</sup>	8497.5	0.64	0.36	6472-6680
MP1	Mt. Palomar	1.5m	1992 Aug 17	08 <sup>h</sup> 05 <sup>m</sup>	8851.8	0.02	1.00	6255-6925
MP2	Mt. Palomar	1.5m	1992 Aug 17	08 <sup>h</sup> 13 <sup>m</sup>	8851.8	0.02	1.00	6255-6925
MP3	Mt. Palomar	1.5m	1992 Aug 18	09 <sup>h</sup> 57 <sup>m</sup>	8852.9	0.06	1.00	6285-6925
MP4	Mt. Palomar	1.5m	1992 Aug 19	10 <sup>h</sup> 04 <sup>m</sup>	8853.9	0.09	1.00	6255-6935
RO1	Rozhen	2.0m	1992 Sep 03	23 <sup>h</sup> 30 <sup>m</sup>	8869.5	0.68	0.10	6530-6589
RO2	Rozhen	2.0m	1992 Oct 09	21 <sup>h</sup> 15 <sup>m</sup>	8905.4	0.04	0.10	6543-6602
RO3	Rozhen	2.0m	1993 Feb 05	17 <sup>h</sup> 40 <sup>m</sup>	9024.2	0.52	0.10	6533-6594
RO4	Rozhen	2.0m	1993 Feb 06	19 <sup>h</sup> 30 <sup>m</sup>	9025.3	0.56	0.10	6534-6594

**Table 4.** Observed H $\alpha$  line parameters of LSI+61°303

Id.	$v_r$ (B) (km s <sup>-1</sup> )	$v_r$ (dip) (km s <sup>-1</sup> )	$v_r$ (R) (km s <sup>-1</sup> )	FWHM(B) (Å)	FWHM(R) (Å)	B/R	-EW(H $\alpha$ ) (Å)	EW(wings) (Å)	EW(R)/EW(B)
AS1	-227	-50	154	5.10	6.85	1.14	11.46	1.96	0.79
AS2	-208	-62	130	5.57	8.67	1.18	6.26	0.61	0.73
AS3	-228	-56	125	5.13	6.48	1.25	6.20	0.95	0.89
AS4	-219	-52	139	4.64	7.11	1.14	7.14	0.88	0.72
AS5	-223	-69	137	4.64	6.90	1.17	9.82	0.96	0.72
LP1	-152	8	177	7.14	5.64	0.83	14.22	2.21	0.99
LP2	-221	-64	110	5.15	5.10	0.74	15.49	2.68	0.71
LP3	-230	-72	108	5.20	5.48	0.86	13.09	3.45	0.87
MP1	-99	41	202	6.32	5.52	0.78	16.22	2.32	0.84
MP2	-96	35	205	5.10	5.79	0.83	17.02	2.60	0.74
MP3	-161	-17	130	5.49	5.43	1.03	12.69	1.59	1.00
MP4	-191	-34	132	4.64	4.91	1.04	15.43	1.43	0.89
RO1	-209	-69	110	4.55	6.68	0.79	18.50	-	0.64
RO2	-193	-46	130	3.65	5.27	0.95	12.13	-	0.60
RO3	-215	-88	83	5.55	5.52	0.71	10.42	-	0.54
RO4	-184	-76	105	5.57	5.15	0.77	11.69	-	0.68

February-March 1978. Our data confirm this variation of radial velocity. We also find that the central dip has  $v_r > 0$  km s<sup>-1</sup>, but only in two low resolution spectra. A global shift of the H $\alpha$  line is probably  $\lesssim 60$  km s<sup>-1</sup>, if we neglect the three "outsider" points that come from low resolution, low significance observations. A weighted average of the radial velocities over the inverse square of dispersion yields  $v_r$ (B)  $\approx -208$  km s<sup>-1</sup>,  $v_r$ (dip)  $\approx -60$  km s<sup>-1</sup>. The variation in the peak separation may be due to an increase in  $v_r$  of the red peak and a decrease in the  $v_r$  of the blue peak.

### 5.2. Line width and B/R variability

In Fig. 8 we represent the FWHM(R) and FWHM(B) as a function of radio phase, while Fig. 9 illustrates the B/R peak ratio and EW(H $\alpha$ ) as a function of radio phase also.

The H $\alpha$  profile of LSI+61°303 is not peculiar with respect to those observed in other Be stars (we can, for instance, com-

pare LSI+61°303 to the Be stars studied by Slettebak et al. (1992)). The EW(H $\alpha$ ) of LSI+61°303 is  $\lesssim 20$  Å. This value sets LSI+61°303 among the H $\alpha$ -weak Be stars. However, the value of the H $\alpha$  FWZI is, to the best of our knowledge, among the largest values observed in Be stars.

Gregory et al. (1979) described LSI+61°303 as having Balmer line emission of variable profile intensity and decrement. Later, HC81 showed that the radial velocity of the central dip, the emission intensity, and the peak ratio were all phase related quantities. The H $\alpha$  line profile did not change in its main features over 14 years. The stability of the H $\alpha$  profile is undoubtedly remarkable, since Be stars sometimes exhibit strong H $\alpha$  profile changes over timescales of several months. Our data confirm that the H $\alpha$  EW changes strongly in correspondence of the radio outburst. The minimum value of EW (6 Å) and the maximum value of peak ratio B/R are observed between radio phase 0.7-0.8 (see Fig. 9).

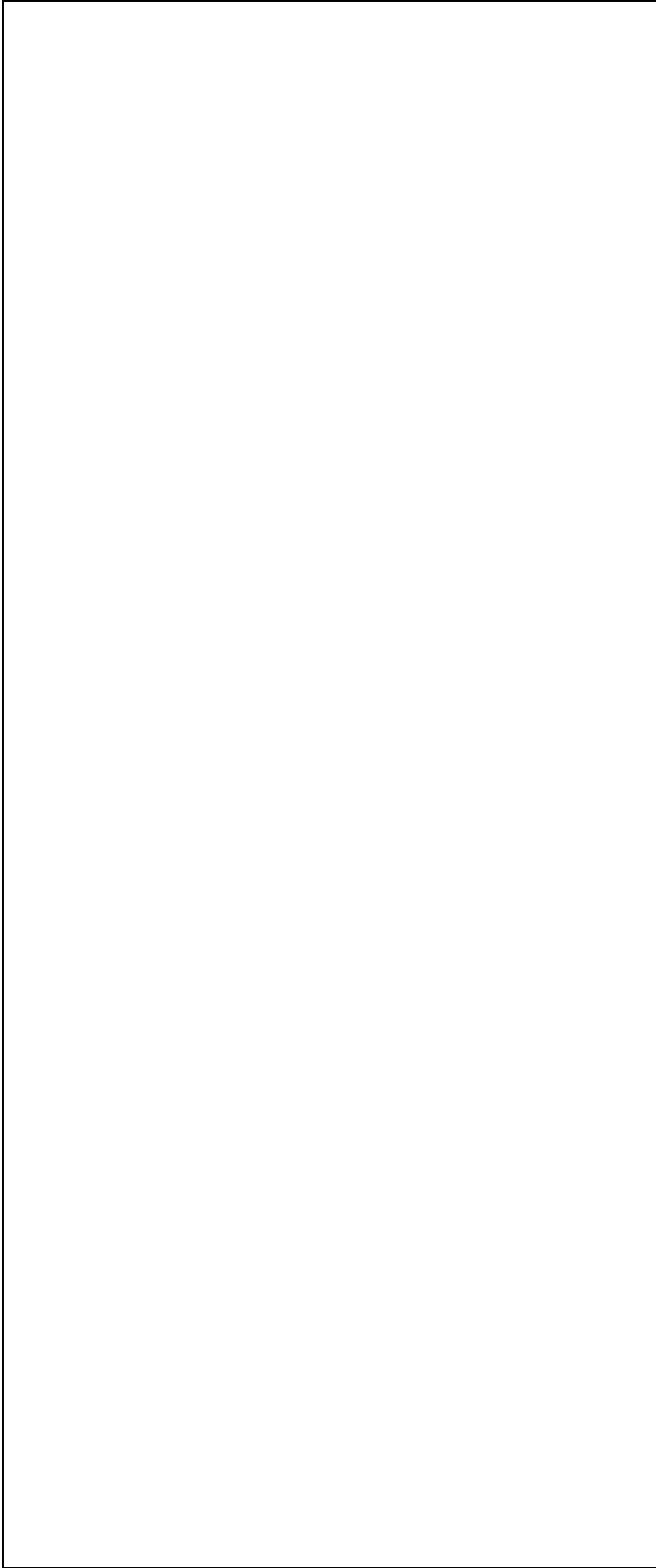


**Fig. 6.** Normalized  $H\alpha$  line profiles of LSI+61°303 at different radio phases given on right-hand side. Horizontal scale is wavelength in Å and vertical scale is in arbitrary intensity units. The Rozhen Observatory spectra have been convolved with a gaussian of FWHM = 0.3 Å. Identification codes are revealed in Table 3.

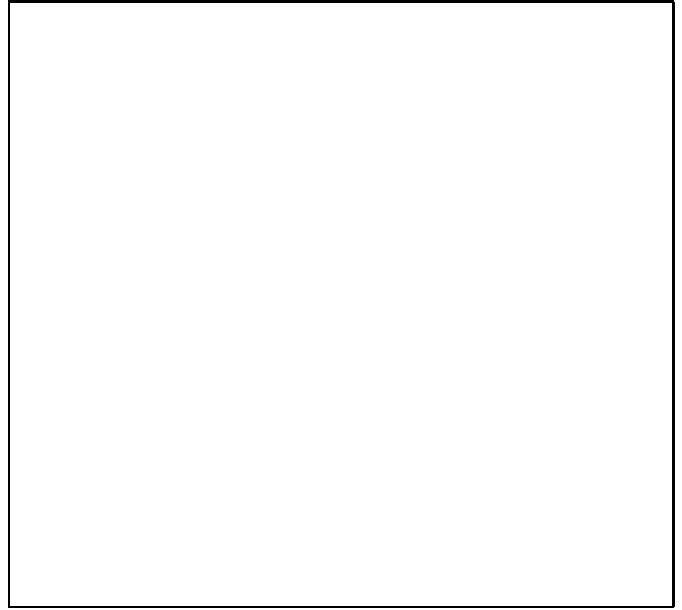


**Fig. 7.** Radial velocity difference, between the R and B peaks, and heliocentric radial velocity of the central dip. Both are in  $\text{km s}^{-1}$  and horizontal axis is labeled in radio phase. The size of the dots is proportional to the dispersion, i.e., the larger the dot, the higher the reliability of the measurement.

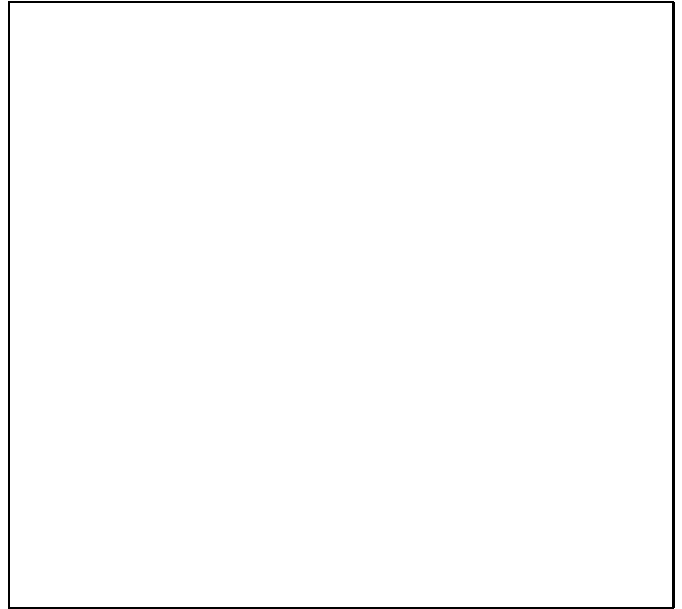


**Fig. 8.** FWHM(R) and FWHM(B) as a function of radio phase. Black dots represent the FWHM of the fitting gaussians and white dots correspond to the hump half maximum width. The size of the dots is proportional to the dispersion.



**Fig. 9.** B/R peak ratio and EW(H $\alpha$ ) in Å as a function of radio phase.

As can be seen in Fig. 8, the FWHM(R) increases from a value of  $\sim 6$  Å ( $\sim 250$  km s $^{-1}$ ), at radio phase  $\sim 0.5$ , to a value of  $\sim 8$  Å ( $\sim 350$  km s $^{-1}$ ) at radio phase  $\sim 0.7$ . So, the red hump seems to become substantially broader near the time of radio maximum. On the contrary, the FWHM(B) appears to decrease slightly at the same time. In the Asiago spectra (obtained close to the radio maximum), the FWHM of the red hump is visibly larger by  $\approx 100$  km s $^{-1}$  than that of the blue one. The exact values of the line width depends somewhat on the method employed for the measurement. To ascertain that this effect is real we also measured directly the half width of the two humps. Although the numbers are somewhat different, the same effect is evident in Fig. 8. Also, we have computed the flux ratio of the blue and red hump, which happens to be  $\lesssim 1$  at all epochs of observation. This implies that the change in peak intensity ratio is mainly due to a variation in width of the red hump.

The flux ratio between line core and line wings is relatively constant in all spectra ( $\sim 0.15$ ) but LP3. The H $\alpha$  profile in LP3 displays a prominent blue wing, with EW(wings)/EW(core)  $\sim 0.26$ , and asymmetry index of the line wings AI  $\sim -0.37$ , where AI is defined as [EW(Blue Wing) - EW(Blue Wing)]/EW(Both Wings). In the other low resolution observations, the H $\alpha$  line wings are symmetric within the uncertainties.

### 5.3. Spectroscopic discussion

The most widely accepted explanation of the H $\alpha$  line profiles in Be stars involves a circumstellar disk-like envelope that produces the double-peaked line core. Electron scattered H $\alpha$  photons are expected to produce extended line wings. The FWZI of LSI+61 $^{\circ}$ 303 H $\alpha$  is  $\approx 3100$  km s $^{-1}$   $\gg 2v \sin i \sim 780$ – $960$  km s $^{-1}$  (HC81). The excess in the line wings is especially evident if we model the core as a sum of two gaussians (FWZI(core)  $\approx 1000$  km s $^{-1}$ ). If we assume that the line core is emitted in a disk, and that the velocity field in the disk is ke-

plerian, we can estimate the ratio between the inner and outer radius of the disk. We obtain  $R_{out}/R_{in} \approx 9.2$ , for FWZI(core)  $\approx 1000$  km s $^{-1}$ . The electron scattering optical depth  $\tau_{es}$  for a disk-like geometry can also be computed. The density was assumed to depend upon  $r$  as  $n_e = n_{e,0}(r/R_{in})^{-\alpha}$ , and to fade exponentially above and below the symmetry plane of the disk. For  $n_{e,0} = 10^{12}$  cm $^{-3}$ , and for  $\alpha = 2$ , we find that  $\tau_{es} \gtrsim 0.3$ , and, if the density  $n_{e,0}$  is  $\gtrsim 10^{12}$  cm $^{-3}$ ,  $\tau_{es} \sim 1$ . If  $\tau_{es}$  is so large, and if the temperature of the gas is  $T_e \gtrsim 10^4$  K, as likely, extended line wings of FWZI  $\sim 3000$  km s $^{-1}$  can be produced (Poeckert & Marlborough, 1979).

The circumstellar disk around the B star should have  $R_{out} \sim 5 \times 10^{12}$  cm, a value similar to the length of the semi-major axis of the orbit estimated by HC81. If the eccentricity is  $\approx 0.75$ , the secondary star should cross the circumstellar disk and, if the circumstellar disk itself is nearly coplanar to the plane of the orbit, even sweep across it while close to periastron. The resultant accretion could produce the radio outburst. A similar model has been proposed for the Be star/X-ray binary systems A0538–66 and V0332+52 (e.g., Slettebak, 1988). The increase in width of the red hump could be due to a non-axisymmetric perturbation in the circumstellar disk, occurring close to the outer edge of the disk. For instance, the secondary may be crossing the circumstellar shell at that time, close to its outer radius (it is interesting to note that the blue hump is probably wider than the red one at radio phase  $\approx 0.4$ ). However, the orbital solution of HC81 suggests that the broadening is occurring when the star is close to apoastron, where the secondary is probably not in contact with the circumstellar disk of the Be star, if the radius of the circumstellar disk is  $R_{out} \approx 5 \times 10^{12}$  cm.

Alternatively, most of the H $\alpha$  emission could be associated with the compact secondary. An accretion disk around a  $\sim 1$  M $_{\odot}$  compact object would have  $R_{out} \sim 1 \times 10^{12}$  cm, without considering broad wings produced by electron scattering. The strong decrease in the H $\alpha$  EW at radio maximum can be explained either in terms of obscuration of the disk by the Be star (Mendelson & Mazeh, 1989), or in terms of reduced emissivity in the disk.

The JHK light curves point toward an eclipsing binary. Hence, the plane of the orbit should be close to the line of sight. Since the secondary has probably a mass of only 1/6 or less the mass of the primary, we expect also a large radial velocity oscillation in the peak positions ( $\sim 300$  km s $^{-1}$ ). Our radial velocity data are not consistent with this, nor are the data obtained by the previous investigators.

Less clear is the interpretation of the variation of the wings; we think that a set of homogeneous observations of sufficiently high S/N and resolution are needed to finally reject the possibility that the line wings might be emitted by the accretion disk of the secondary.

Even if the accretion disk around the compact star does not emit the bulk H $\alpha$  luminosity, the increase in FWHM(R) and in  $\Delta v_r = v_r(R) - v_r(B)$  may be caused by an unresolved component whose radial velocity reaches a maximum in correspondence to the radio maximum. We may expect this if, for instance, a cloud of line emitting gas would be ballistically ejected along the secondary disk axis. This suggestion is appealing, since the radial velocity of this unseen component should be  $\gtrsim 200$  km s $^{-1}$  at radio maximum, consistent with the velocity of the bipolar ejecta of radio plasma partially resolved with VLBI techniques by Massi et al. (1993). A strong



analogy could be envisaged with the model proposed by Martin & Rees (1979) for SS433. Present data on radial velocity and FWHM variation can be explained by a combination of global line displacement due to the orbital motion of the Be star, and of the  $v_r$  variation of this unresolved component. The red shoulder often present in the H $\alpha$  profile could be a related, higher velocity, feature.

## 6. Conclusions

Our Johnson photometric monitoring of LSI+61°303 has shown that this object presents a  $\sim 26$  d periodic modulation in the V band. The shape and amplitude of this modulation are similar to those found by Mendelson & Mazeh (1989). In addition, the J, H and K observations reported in this paper have revealed, for the first time, new evidence of infrared variability with similar trends as seen in the optical, but with higher amplitude ( $0^m.2$ ). We have established also that the merged JHK light curve exhibits a modulation with period similar to the radio period. A possible interpretation of this periodicity could involve the eclipse and attenuation of the secondary star emission by the Be primary and its envelope.

It is unclear whether an accretion disk around a compact, degenerate companion may contribute to the H $\alpha$  emission, or whether the variations observed are due to perturbations produced by the companion on the circumstellar disk of the Be primary. This problem persists also because Be stars, as a class, are far from being well understood. LSI+61°303 clearly deserves more observations from ground and space. Monitoring of the H $\alpha$  profile at high and intermediate resolution will help to solve the main ambiguities left by the present investigation. It is also desirable to obtain a new spectroscopic orbital solution.

*Acknowledgements.* We thank all observers who also collaborated in the observations, especially Mauro D' Onofrio & Gabriele Cremonese for the spectra obtained at the Asiago Observatory, and for help during part of the spectroscopic data reduction. We also thank R. Canal for valuable comments as well as F. Comerón and M. Fernández for participating in some photometric observations. JMP, JM, FF, CJ and JT acknowledge partial support by CICYT (ESP93-1020-E) and DGICYT (PB91-0857). Extragalactic Astronomy at the University of Alabama is supported under EPSCOR Grant R11-8996152. The TCS is operated on the island of Tenerife by the Instituto de Astrofísica de Canarias (IAC), in the Spanish Observatorio del Teide. The 1.5 m telescope at Palomar Mt. is jointly owned by California Institute of Technology and the Carnegie Institute of Washington. The CAHA 1.23 m telescope is operated by Max Planck Institute für Astronomie. The INT and JKT are operated on the island of La Palma by the Royal Greenwich Observatory in the Spanish ORM of the IAC. We also thank the staff of the OAN 1.5 m telescope. Much of the data were analysed using the Southampton University Starlink node which is founded by the SERC. CE acknowledges the support of an SERC Studentship. We are also grateful for the support of the ING Service Programme that provided some of the data for this work.

## References

- D'Amico N., Lorenzetti D., Massaro E., Saraceno P., Strafella F., 1987, A&A 180,114  
 Bartolini C., Custodi P., Dell'Atti F., Guarnieri A., Piccioni A. 1983, A&A, 118, 365  
 Bignami G.F., Caraveo P.A., Lamb R.C., Markert T.H., Paul J.A. 1981, ApJ, 247, L85  
 Elias J.H., Matthews K., Neugebauer G., Soifer B.T., 1985, AJ 90, 1188  
 Estalella R., Paredes J.M., Rius A., Martí J., Peracaula M. 1993, A&A, 268, 178  
 Gregory P.C., Taylor A.R. 1978, Nat, 272, 704  
 Gregory, et al., 1979, AJ 84, 1030  
 Gregory P.C., Huang-Jian Xu, Backhouse C.J., Reid A. 1989, ApJ, 339, 1054  
 Hermsem W., Swanenburg, B.N., Bignami G.F. et al. 1977, Nat, 269, 495  
 Hutchings J.B., Crampton D. 1981, PASP, 93, 486  
 Lipunova N.A. 1988, Sov. Astron., 32, 52  
 Martí J., Paredes J.M., 1994 (in preparation)  
 Martin P.G., & Rees, M. J., 1979, MNRAS 189, 19P  
 Massi M., Paredes J.M., Estalella R., Felli M. 1993, A&A, 269, 249  
 Mendelson H., Mazeh T. 1989, MNRAS, 239, 733  
 Paredes J.M., Figueras, F. 1986, A&A, 154, L30  
 Paredes J.M. 1987, RMAA, 14, 395  
 Paredes J.M., Estalella R., Rius A. 1990, A&A, 232, 377  
 Paredes J.M., Martí J., Estalella R., Sarrate J. 1991, A&A, 248, 124  
 Perotti F., Della Ventura A., Villa G., Di Cocco G., Butler R.C., Dean A.J., Hayles R.I. 1980, ApJ, 239, L49  
 Poeckert, R., & Marlborough, J. M., 1979, ApJ 233, 259  
 Slettebak A., 1979, Space Sci. Rev., 23, 541  
 Slettebak A., 1988, PASP 100,770  
 Slettebak A., Collins G.W.II, Truax R., 1992, ApJS 81, 335  
 Smirnov O.M., Piskunov N.E., Afanasyev V.P., Morozov A.I., 1992, *Astronomical Data Analysis Software and Systems I*, ASP Conference Series, vol. 26, eds. Worrall D.M., Biemesderfer C., Barners J., ASP, San Francisco, 344  
 Stellingwerf R.F., 1978 ApJ, 224, 953  
 Taylor A.R., Gregory P.C. 1982, ApJ, 255, 210  
 Taylor A.R., Gregory P.C. 1984, ApJ, 283, 273  
 Taylor A.R., Kenny H.T., Spencer R.E., Tzioumis A., 1992, ApJ, 395, 268